nature catalysis

Article

https://doi.org/10.1038/s41929-025-01453-z

Excited-state configuration controls the ability of nitroarenes to act as energy transfer catalysts

Received: 12 February 2025

Accepted: 29 October 2025

Published online: 17 December 2025

Check for updates

Martin Rihtaršič[1,3], Byeongseok Kweon[1,2,3], Piotr T. Błyszczyk[1], Alessandro Ruffoni[1], Enrique M. Arpa[1] ✉ & Daniele Leonori[1] ✉

Energy transfer (EnT) catalysis enables the selective population of triplet excited states without previous singlet excitation, thus eliminating the need for high-energy irradiation. Traditionally, EnT catalysis has been approached by developing specific photosensitizers with triplet energies (E_T) that match those of the targeted substrates. Here we introduce an alternative approach to EnT using widely available nitroarenes as photocatalysts. Our findings reveal that their catalytic efficiency is governed by the localization of their excited state rather than E_T. Specifically, $^3\pi,\pi^*$ nitroarenes, where the excitation is centred on the aromatic core rather than the nitro group, exhibit superior catalytic performance compared with their $^3n,\pi^*$ counterparts. We have demonstrated the utility of this concept for nitroarene photocatalysis in contra-thermodynamic *E*-to-*Z* alkene isomerization and [2 + 2] cycloadditions. Additionally, we use the energetic descriptor ΔE_{TT} as easy tool to distinguish the preferential population of $^3n,\pi^*$ versus $^3\pi,\pi^*$ triplet states and therefore accelerate the identification of novel photosensitizers.

The population of electronically excited states enables reactivity patterns that are inaccessible in the ground state[1,2]. However, direct photoexcitation of organic molecules is often hindered by their low absorbance profiles which requires the use of high-energy irradiation (for example, UV-B). This requires the use of specialized equipment and can compromise compatibility with many functional groups[3,4]. Energy transfer (EnT) catalysis offers a powerful alternative by directly populating triplet excited states (T_1), bypassing the higher-energy singlet states (S_1) and using irradiation wavelengths outside the substrate's ground-state absorbance profile[3,5–7]. In EnT catalysis, a photocatalyst functions as a light-harvesting system, transferring energy to the substrate through a Dexter energy transfer mechanism[8] (Fig. 1a). Effective photosensitizers are defined by several key properties: an absorption profile suitable for low-energy irradiation (preferably visible light), strong spectral overlap with the substrate's absorption spectrum, high intersystem crossing (ISC) quantum yield, and a long-lived triplet state to facilitate bimolecular quenching[5]. Importantly, the triplet energy (E_T) of the photocatalyst must exceed that of the substrate to drive an exergonic EnT process.

Recent developments in EnT catalysis have focused on designing both transition metal and organic photosensitizers where fine-tuning of their structural features modulates their E_T and expands their synthetic utility[9–14]. In this study, we introduce an alternative approach to EnT catalysis in which the sensitization process is governed by the nature of the excited-state configuration. By switching the localization of the excited state within the photosensitizer we demonstrate the effective use of nitroarenes—some of the simplest and most abundant feedstocks—as versatile EnT photocatalysts (Fig. 1b). This strategy establishes the use of nitroarenes as catalysts and provides a practical alternative to systems reliant on precious metals or synthetically demanding scaffolds.

Results

E-to-*Z* isomerization of cinnamates

Our group and others have recently demonstrated the ability of triplet nitroarenes to participate in various synthetically valuable transformations, such as the oxidative cleavage of alkenes, C(sp^3)–H oxidation, and aromatic ring expansion and contraction reactions[15–22] (Fig. 1b). Upon photoexcitation, nitroarenes populate the T_1 state, characterized

[1]Institute of Organic Chemistry, RWTH Aachen University, Aachen, Germany. [2]Institute for Organic Chemistry, University of Münster, Münster, Germany. [3]These authors contributed equally: Martin Rihtaršič, Byeongseok Kweon. ✉e-mail: enrique.arpa@rwth-aachen.de; daniele.leonori@rwth-aachen.de

https://doi.org/10.1038/s41929-025-01453-z

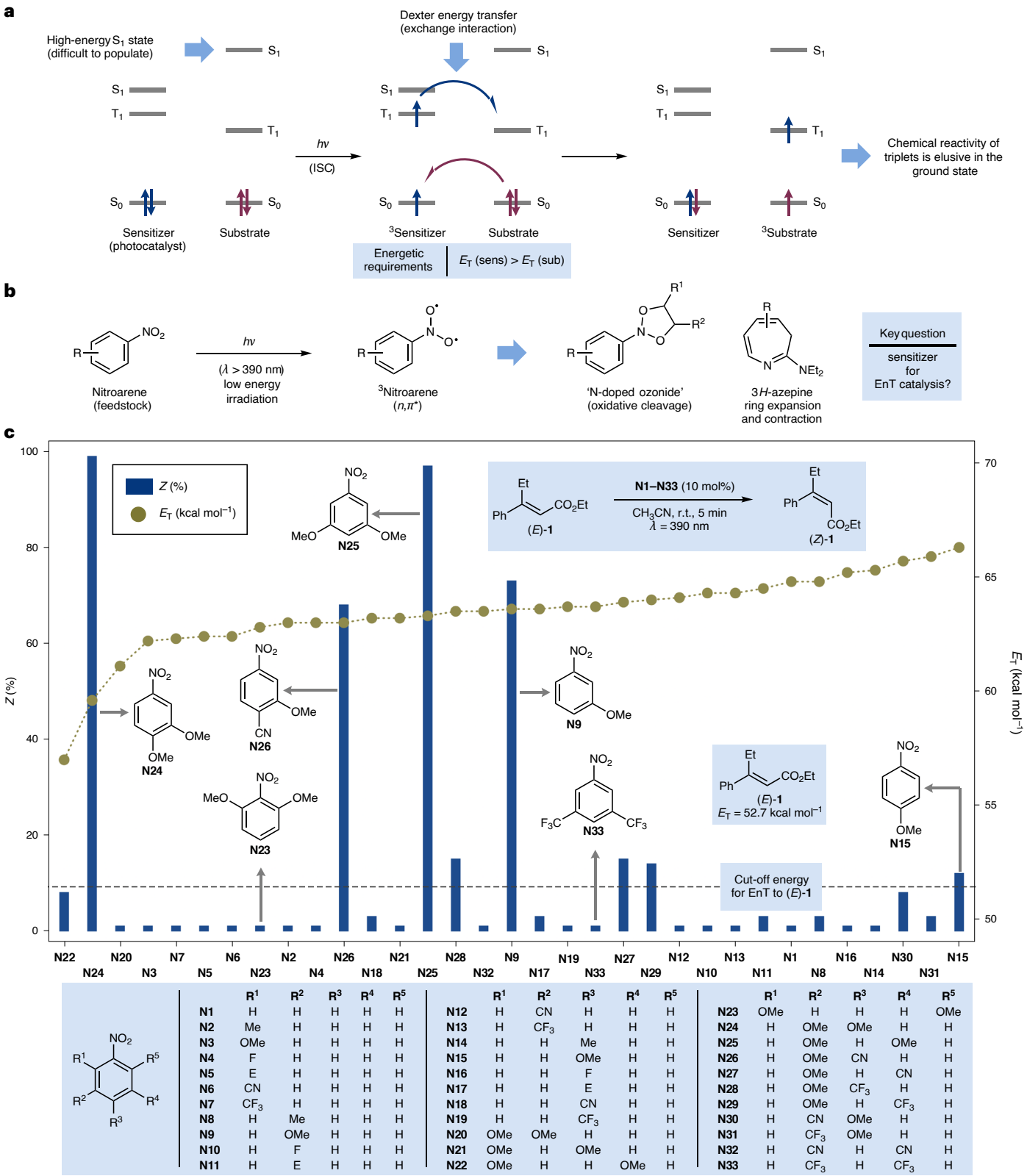

	R1	R2	R3	R4	R5
N1	H	H	H	H	H
N2	Me	H	H	H	H
N3	OMe	H	H	H	H
N4	F	H	H	H	H
N5	E	H	H	H	H
N6	CN	H	H	H	H
N7	CF_3	H	H	H	H
N8	H	Me	H	H	H
N9	H	OMe	H	H	H
N10	H	F	H	H	H
N11	H	E	H	H	H
N12	H	CN	H	H	H
N13	H	CF_3	H	H	H
N14	H	H	Me	H	H
N15	H	H	OMe	H	H
N16	H	H	F	H	H
N17	H	H	E	H	H
N18	H	H	CN	H	H
N19	H	H	CF_3	H	H
N20	OMe	OMe	H	H	H
N21	OMe	H	OMe	H	H
N22	OMe	H	H	OMe	H
N23	OMe	H	H	H	OMe
N24	H	OMe	OMe	H	H
N25	H	OMe	H	OMe	H
N26	H	OMe	CN	H	H
N27	H	OMe	H	CN	H
N28	H	OMe	CF_3	H	H
N29	H	OMe	H	CF_3	H
N30	H	CN	OMe	H	H
N31	H	CF_3	OMe	H	H
N32	H	CN	H	CN	H
N33	H	CF_3	H	CF_3	H

Fig. 1 | EnT catalysis using triplet nitroarenes. a, EnT photocatalysis exploits the ability of triplet sensitizers to transfer their energy to the substrate, providing it has a lower E_T. **b**, Nitroarenes can be photoexcited to their triplet states using visible light. These species can be used in many processes but their ability to be employed as photocatalysts in EnT remains unexplored. **c**, *E*-to-*Z* photoisomerization efficiency of cinnamate (*E*)-**1** for all the tested nitroarenes sorted by increasing triplet energy (E_T). The adiabatic energy for the lowest-lying triplet state of each nitroarene was calculated at the M06-2X/cc-pVTZ/SMD(MeCN)//M06-2X/cc-pVDZ level of theory. Et, ethyl; Me, methly; Ph, phenyl.

https://doi.org/10.1038/s41929-025-01453-z

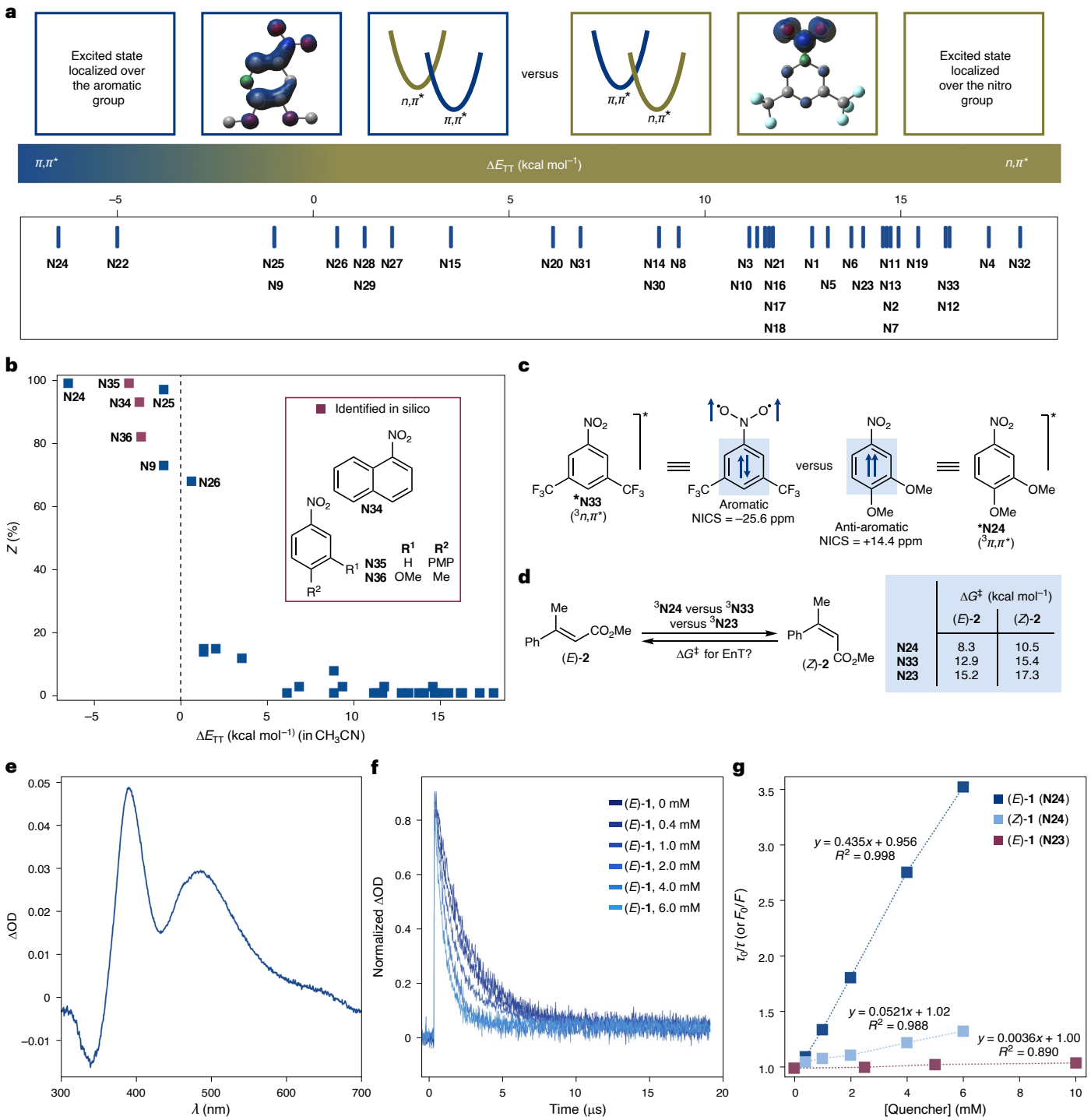

Fig. 2 | Mechanistic studies for triplet nitroarene-catalysed *E*-to-*Z* isomerizations. a, Top: spin densities of $^3\pi,\pi^*$ (**N24**) and $^3n,\pi^*$ (**N33**); bottom: scale of ΔE_{TT} values of **N1**–**N33**. Red, oxygen; grey, carbon; blue, nitrogen; cyan, fluorine; hydrogens omitted for clarity. **b**, Contra-thermodynamic *E*-to-*Z* isomerization of (*E*)-**1** with **N1**–**N33** plotted against their ΔE_{TT} values. **c**, Calculated nucleus-independent chemical shifts, NICSzz(1), values for selected $^3\pi,\pi^*$ (**N24**) and $^3n,\pi^*$ (**N33**) nitroarenes at the M06-2X/cc-pVTZ/SMD(MeCN)//M06-2X/cc-pVDZ level of theory. **d**, Activation barriers for EnT using Marcus theory calculated at the M06-2X/cc-pVTZ/SMD(CH_3CN)//M06-2X/cc-pVDZ level of theory. **e**, Transient absorption spectrum for **N24** in deaerated CH_2Cl_2 (λ_{exc} = 355 nm). **f**, Normalized transient decay traces for **N24** in deaerated CH_2Cl_2 (λ_{exc} = 355 nm) monitored at 390 nm upon addition of increasing amounts of (*E*)-**1**. In all cases, the decays were fitted to a monoexponential function. **g**, Stern–Volmer plots for quenching of photoexcited **N24** by (*E*)-**1**, **N24** by (*Z*)-**1**, and **N23** by (*E*)-**1**. PMP, *para*-methoxyphenyl.

by a distinct $^3n,\pi^*$ configuration, localized on the NO_2 group causing loss of its planarity. This excited-state geometry causes the nitro group to behave as a double oxygen radical species that can engage in radical-type cascade reactions with alkenes[15–17], activated C(sp^3)–H bonds[18,19] and P(III) reagents[20–22]. So far, triplet nitroarenes have been used in stoichiometric reactivity modes resulting in their conversion into other chemical species. We recently became interested in understanding if their triplet character could also be exploited in catalytic

https://doi.org/10.1038/s41929-025-01453-z

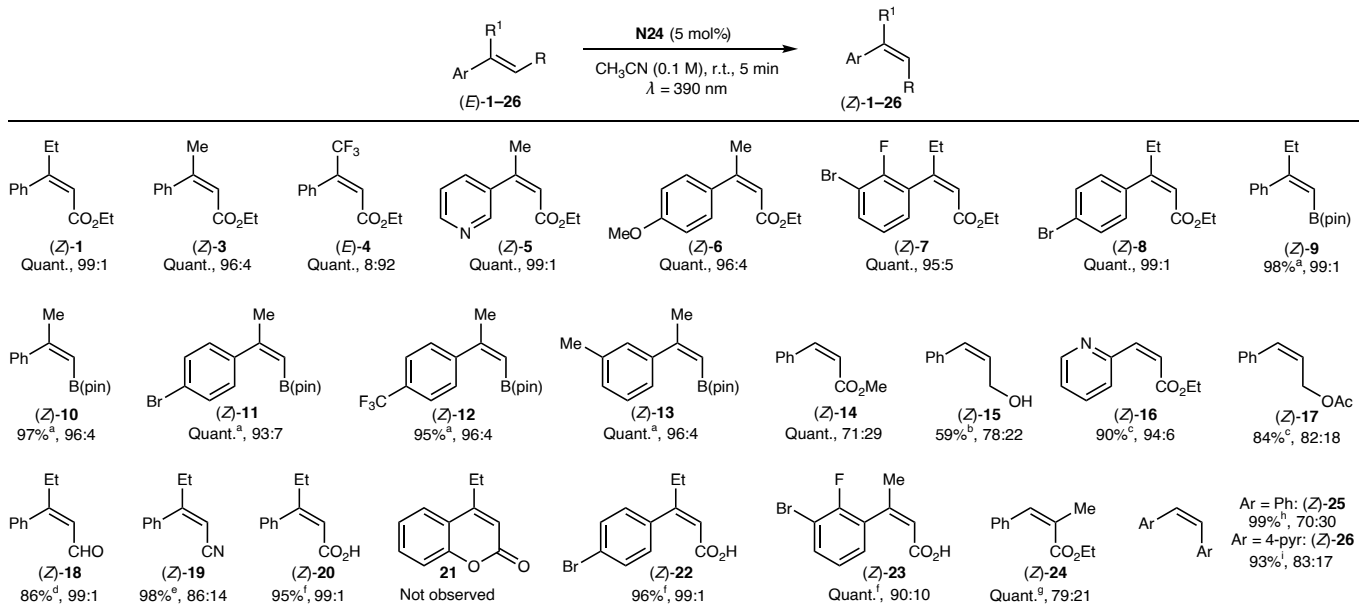

Fig. 3 | Scope for the triplet nitroarene-catalysed *E*-to-*Z* isomerizations. [a]**N24** (10 mol%), CH_3CN (0.03 M), 1-h reaction time. [b]**N34** (10 mol%), CH_3CN (0.05 M), 60-h reaction time. [c]**N24** (10 mol%), CH_3CN (0.05 M), 6-h reaction time. [d]**N24** (10 mol%). [e]**N24** (10 mol%), 10-min reaction time. [f]**N24** (10 mol%), CH_3CN (0.05 M), 30-min reaction time. [g]**N35** (10 mol%), 1-h reaction time. [h]**N24** (20 mol%), 10-min reaction time. [i]**N24** (20 mol%), 16-h reaction time. Ar, aryl; Ac, acetyl; pin, pinacolato; pyr, pyridine; quant., quantitative.

applications for EnT[23–25]. Given the wide commercial availability of nitroarenes, we were intrigued by the potential to tailor their reactivity by rational modification of their substitution patterns. Moreover, nitroarenes possess favourable properties for such applications, including strong absorption in the UV-A/visible range and highly efficient ISC ($\Phi \approx 0.8$)[26].

We initiated this study by investigating the contra-thermodynamic *E*-to-*Z* isomerization of cinnamate (*E*)-**1**, a process for which the current state-of-the-art utilizes several types of photocatalysts, generally over extended reaction times (~24 h)[27–31]. Leveraging the broad availability of nitroarenes, we rapidly screened a wide range of mono- and disubstituted systems (**N1**–**N33**, 10 mol%) (Fig. 1c). Pleasingly, we found that the desired isomerization could be achieved with several reagents under irradiation with purple light-emitting diodes (LEDs, $\lambda = 390$ nm) at room temperature in CH_3CN solvent. Pleasingly, the reaction times were reduced to just a few minutes, demonstrating the high catalytic efficiency of some specific triplet nitroarenes.

A particularly intriguing finding was the dramatic variation in catalytic performance among different nitroarenes based on their substitution patterns. For example, 3,5-$(CF_3)_2$-nitroarene **N33**, which is highly effective in the oxidative cleavage of alkenes[15], showed no capacity for isomerization. In contrast, substrates bearing electron-donating OMe groups—typically unreactive in this transformation—exhibited good-to-excellent reactivity. Specifically, *p*-substituted **N15** achieved 12% *Z* isomerization, while the *m*-substituted **N9** increased this to 73%. Derivatives featuring two OMe groups performed best, with *m*,*m*-functionalized **N25** yielding 97% *Z* isomerization and the *m*,*p* derivative **N24** emerging as the optimal catalyst, achieving a *Z*:*E* ratio of 99:1. All reactions tested resulted in quantitative mass balances.

Investigating differences in EnT efficiency

To understand the varying EnT effectiveness of these nitroarenes, we recorded their UV/visible absorption spectra, confirming they could all be photoexcited with purple LEDs (Supplementary Fig. 4). We then used computational chemistry to calculate their triplet energies. This study revealed that all nitroarenes have similar E_T values, in the range of $E_T = 57–67$ kcal mol^{-1}, which makes them energetically similar to the widely used [Ir(dF(CF_3)ppy)$_2$(dtbbpy)(PF_6)] ($E_T = 61.8$ kcal mol^{-1})[32] and in most cases superior to many commonly used organic dyes such as 4CzIPN ($E_T = 58.3$ kcal mol^{-1})[33]. Interestingly, although the E_T of all nitroarenes is higher than that of (*E*)-**1** ($E_T = 52.5$ kcal mol^{-1}), implying favourable energetic profiles, stark differences in catalytic reactivity were observed. This unexpected outcome challenges the current understanding of EnT catalysis, which largely emphasizes the energetic alignment of excited states as the primary determinant for sensitization.

To better understand the photochemical behaviour of nitroarenes, we conducted additional computational investigations aimed at characterizing their excited-state geometries (Supplementary Table 1). This analysis revealed that the excited-state configurations of these species changed on the basis of their substitution patterns. Specifically, photoexcited nitroarenes can populate either $^3n,\pi^*$ or $^3\pi,\pi^*$ triplet states, differing in the localization of the unpaired electrons: the nitro group for $^3n,\pi^*$ and the aromatic ring for $^3\pi,\pi^*$ (ref. 34; Fig. 2a). To quantify the energetic preference between these states, we used the descriptor $\Delta E_{TT} = E_T(^3\pi,\pi^*) - E_T(^3n,\pi^*)$ and used this energetic parameter to construct an excited-state configuration scale. According to this scale, nitroarenes with $\Delta E_{TT} > 0$ preferentially populate the $^3n,\pi^*$ state, and those with $\Delta E_{TT} < 0$ preferentially populate the $^3\pi,\pi^*$ state. Plotting reaction efficiency against ΔE_{TT} revealed two distinct reactivity clusters: the $^3\pi,\pi^*$ nitroarenes were associated with high *E*-to-*Z* isomerization, while the $^3n,\pi^*$ exhibited low or no reactivity (Fig. 2b).

We wondered whether we could leverage this classification to identify new nitroarenes active in EnT photocatalysis. An in silico screen of several other nitroarenes allowed us to identify three additional $^3\pi,\pi^*$ species not included in our initial screening (**N34**, $\Delta E_{TT} = -2.4$ kcal mol^{-1}; **N35**, −3.0 kcal mol^{-1}; and **N36**, −2.3 kcal mol^{-1}). These nitroarenes exhibited high *E*-to-*Z* isomerization efficiency (82–99%), validating excited-state configuration as a key predictor EnT reactivity. It should be noted that although **N34** and **N35** are structurally quite different from the nitroarenes studied initially, they were nonetheless classified correctly based on the value of ΔE_{TT}, demonstrating the strength of this index in predicting photosensitizing capabilities.

The stark differences in EnT reactivity between $^3\pi,\pi^*$ and $^3n,\pi^*$ nitroarenes are not fully understood but appear to stem from kinetic factors influencing the sensitization process. One notable difference between these two species is their excited-state lifetimes: $^3\pi,\pi^*$ nitroarenes have notably longer lifetimes ($\tau \approx$ µs) than $^3n,\pi^*$ nitroarenes ($\tau \approx$ ps)[26], which might favour applications in bimolecular processes. However, extending reaction times for $^3n,\pi^*$ nitroarenes (for example, **N33**, up to 6 h) in EnT reactions led to marginal improvements in their isomerization capacity. This behaviour contrasts with their performance in alkene ozonolysis, where longer reaction times lead to higher yields[15].

Furthermore, $^3n,\pi^*$ and $^3\pi,\pi^*$ nitroarenes also exhibit structural differences: $^3n,\pi^*$ nitroarenes have a pyramidalized nitrogen atom, whereas $^3\pi,\pi^*$ nitroarenes adopt a planar geometry. These structural variations can influence sensitization reactivity by affecting the energy required for geometric reorganization. For EnT to occur, $^3n,\pi^*$ nitroarenes must first revert to planarity, whereas $^3\pi,\pi^*$ nitroarenes do not undergo such rearrangement. Consequently, the reorganization energy and activation barrier for EnT are expected to be higher for $^3n,\pi^*$ nitroarenes than for $^3\pi,\pi^*$ nitroarenes.

Another key factor that could influence the contrast in observed reactivity is related to the differences in excited-state aromaticity of the $^3n,\pi^*$ and $^3\pi,\pi^*$ states. Triplet $^3n,\pi^*$ states, exclusively localized over the nitro group, leave the electron density of the phenyl ring nearly unperturbed with respect to the ground state, thus rendering the molecule Hückel aromatic[35]. In complete contrast, the highly delocalized nature of $^3\pi,\pi^*$ states makes them Baird antiaromatic[36]. Therefore, the relief of the excited-state antiaromaticity of $^3\pi,\pi^*$ states might be favouring their reactivity in EnT reactions, a process that cannot take place for $^3n,\pi^*$ states[37,38].

Although we cannot ascertain which of the factors discussed above (excited-state lifetime, structural reorganization, (anti)aromaticity, triplet energy) contributes the most in lowering the activation energies for EnT reactions, we decided to calculate these barriers to corroborate whether our computational methodology can correctly predict the outcome of such reactions. Using the procedure developed by Maseras and co-workers[39], which extends Marcus theory to EnT, we calculated the activation energies for the *E*-to-*Z* and *Z*-to-*E* photoisomerization of cinnamate *E*-**2** using **N24** and **N33** as models for $^3\pi,\pi^*$ and $^3n,\pi^*$ nitroarenes, respectively (Supplementary Table 3). We found that the *E*-to-*Z* isomerization with **N24** has the lowest barrier (Fig. 2d, 8.3 kcal mol^{-1}). All the other calculated barriers are at least 2 kcal mol^{-1} higher, which proves that the most facile process is the contra-thermodynamic *E*-to-*Z* isomerization in the presence of $^3\pi,\pi^*$ nitroarenes.

To further corroborate our understanding of the sensitization process, we performed nanosecond transient absorption spectroscopy studies using laser flash photolysis to monitor the behaviour of several nitroarenes in the presence of (*E*)-**1** and (*Z*)-**1**. The triplet states of these species could be observed using the excitation wavelength $\lambda = 355$ nm and their decay measured through time-resolved experiments. For instance, **N24** produced a transient with an absorption maximum at $\lambda_{max} = 390$ nm and a lifetime of $\tau = 2.8$ µs (Fig. 1e). Stern–Volmer quenching studies in the presence of (*E*)-**1** and (*Z*)-**1** revealed differing bimolecular quenching constants: K_q (*E*)-**1** $= 1.67 \times 10^8$ M^{-1} s^{-1} and K_q (*Z*)-**1** $= 0.22 \times 10^8$ M^{-1} s^{-1}, which account for the observed EnT isomerization reactivity (Fig. 1f,g). Most $^3n,\pi^*$ nitroarenes exhibit shorter lifetimes, making them undetectable via laser flash photolysis in the nanosecond time domain. One exception is **N23** which has a long-lived $^3n,\pi^*$ transient ($\lambda_{max} = 280$ nm and $\tau = 310$ ns). Although the lifetime is sufficiently long for application in triplet sensitization, it was not active in *Z* isomerization under our photocatalytic conditions. Quenching studies of **N23** with (*E*)-**1** yielded a bimolecular quenching constant of 1.2×10^7 M^{-1} s^{-1}, more than an order of magnitude lower than **N24** (Fig. 1g). This is in line with the calculated activation barrier for energy transfer to (*E*)-**2**, which is 6.9 kcal mol^{-1} higher for ^{3}**N23** compared with ^{3}**N24** (Fig. 2d). This further underscores the limited capability of $^3n,\pi^*$ nitroarenes to serve as EnT catalysts despite their potentially matching E_T and also lifetime.

Scope of *E*-to-*Z* isomerization

We then evaluated the generality of the contra-thermodynamic isomerization process using **N24** as the EnT catalyst (Fig. 3). Pleasingly, we successfully engaged a variety of differentially functionalized cinnamate derivatives, with substitutions at both the alkene and aromatic units (**1**, **3**–**7**). In all cases, the processes were quantitative, resulting in high *E*-to-*Z* isomerization efficiency. The aromatic unit could be changed with a pyridine ring (**5**) and with a poly functionalized benzenoid system featuring bromine atoms for further cross-coupling applications (**7**, **8**). Furthermore, we extended the reactivity to *E*-styrenyl pinacol boronic esters (**9**–**13**). The high isomerization observed for the boronates offers a convenient alternative to current methods that use Ir(ppy)$_3$ as the EnT photocatalyst and typically require extended reaction times (for example, 24 h)[40,41]. The EnT could also be applied to derivatives lacking an α-substituted styrenyl unit as demonstrated by the use of acrylate (**14**), cinnamyl alcohol (**15**), pyridyl acrylate (**16**) and cinnamyl acetate (**17**). Notably, for compound **15**, higher isomerization was obtained using **N34**.

This catalytic system could also be successfully applied to the *E*/*Z* isomerization of other cinnamyl derivatives bearing aldehyde (**18**), nitrile (**19**) and carboxylic acid (**20**, **22**, **23**) functionalities. In the case of cinnamic acids, the fact that triplet nitroarenes can undergo EnT but not redox chemistry prevents concomitant coumarin formation (for example, **21** from (*Z*)-**20**)[42]. This results in a different outcome compared with standard EnT photocatalysts that also operate under photoredox conditions. This same characteristic enables compatibility with redox-active functionalities, such as electron-deficient aryl bromides, which could otherwise undergo single-electron transfer reduction[43].

Furthermore, we evaluated the reactivity of β-methylcinnamate (**24**) and stilbenes (**25**, **26**). Derivatives such as **24** are typically challenging in this transformation due to the absence of the critical 1,3-allylic strain between the *ortho* proton of the aryl ring and the α-substituent of the alkene[5,27]. Stilbenes provide lower *E*/*Z* ratios because both the *E* and *Z* isomers have accessible triplet energies for sensitization[6]. Nevertheless, moderate to good levels of isomerization were observed.

As for limitations, we were unable to engage alkyl-substituted acrylates or dialkyl olefins because they feature high triplet energies with negligible difference between the two isomers. This effectively precludes selective accumulation of one isomer over the other[5] (Supplementary Note 13).

Application to other photocatalytic EnT processes

To establish the generality of $^3\pi,\pi^*$ nitroarenes as EnT catalysts, we evaluated their performance in other synthetically relevant transformations[44]. One such example is the photochemical intramolecular [2 + 2] cycloaddition of styrene **27**, which features a pendant olefin (Fig. 4a). Current state-of-the-art methods for this reaction use [Ir(dF(CF$_3$)ppy)$_2$(dtbbpy)(PF$_6$)] or tailor-made flavin as the sensitizer, under blue light irradiation ($\lambda = 402$ nm)[45,46].

Pleasingly, our screening of nitroarenes across a range of ΔE_{TT} values revealed a similar situation whereby reactivity is independent of the matching E_T of the various nitroarenes. This provided the same reactivity trend where $^3\pi,\pi^*$ derivatives consistently demonstrated high reactivity, while $^3n,\pi^*$ nitroarenes exhibited considerably lower reaction efficiency. From this screening, nitroarene **N34** emerged as the optimal catalyst and was used for further mechanistic studies. As illustrated in Fig. 4b, nitroarene photocatalysis enabled the rapid assembly of a series of bicyclic derivatives (**27a**–**33a**). These products spanned a wide range of substitution patterns, including the formation of quaternary centres (**28a**–**34a**), incorporation of both electron-rich

https://doi.org/10.1038/s41929-025-01453-z

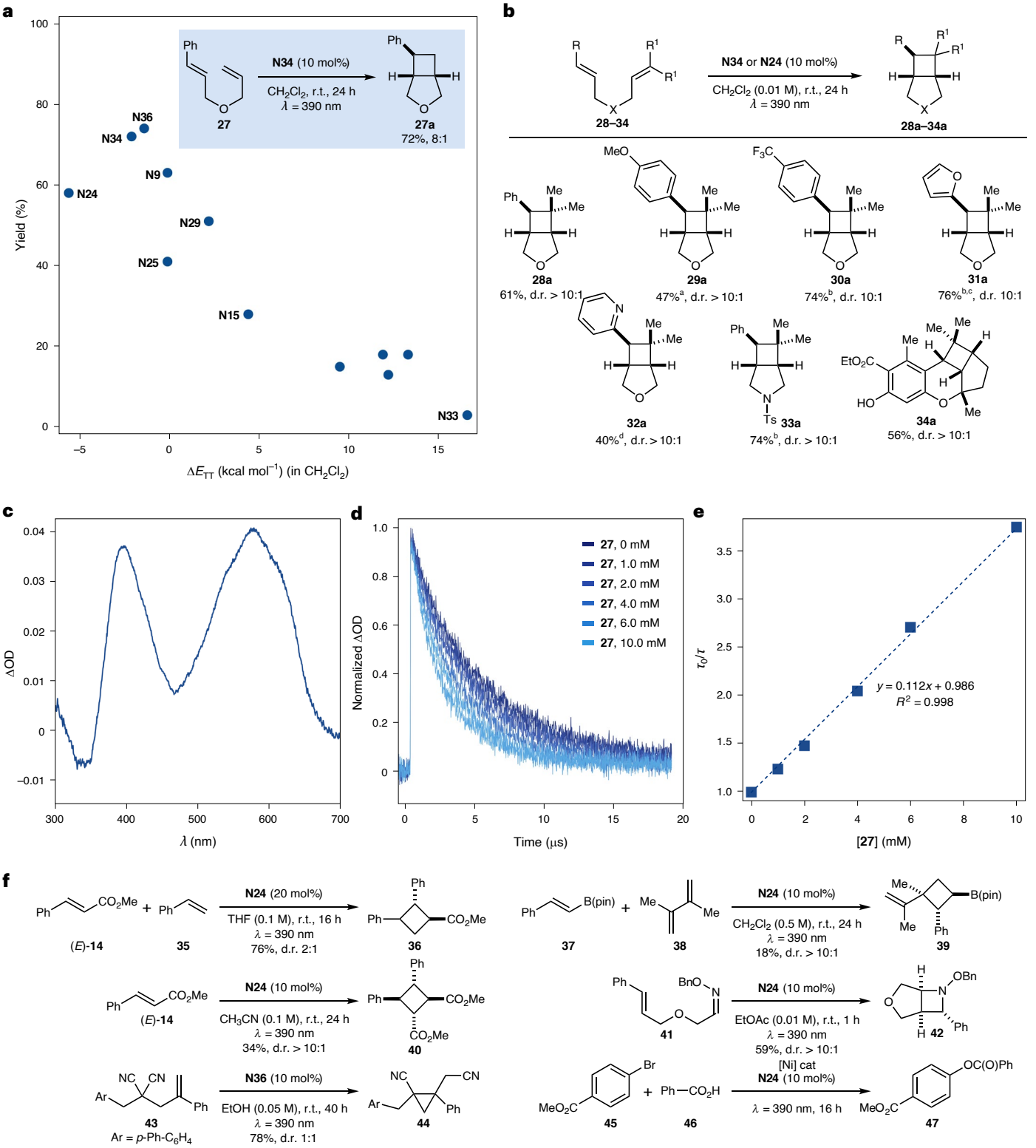

Fig. 4 | Nitroarene photocatalysis can be used in other EnT processes. **a**, Plot of yield versus ΔE_{TT} for the intramolecular [2 + 2] cycloaddition of **27**. **b**, Reaction scope for [2 + 2] cycloaddition. **c**, Transient absorption spectrum for **N34** in deaerated CH_2Cl_2 (λ_{exc} = 355 nm). **d**, Normalized transient decay traces for **N34** in deaerated CH_2Cl_2 (λ_{exc} = 355 nm) monitored at 566 nm upon addition of increasing amounts of **27**. In all cases, the decays were fitted to a monoexponential function. **e**, Corresponding Stern–Volmer plot. **f**, Nitroarene photocatalysis applied to other cycloaddition reactions: [a]**N24** (5 mol%); [b]**N24** (10 mol%); [c]6-h reaction time; [d]**N24** (15 mol%), 48-h reaction time. Bn, benzyl; THF, tetrahydrofuran; Ts, tosyl.

furan (**31a**) and electron-poor pyridine (**32a**) residues, and the assembly of structurally complex tetracyclic derivative (**34a**), an intermediate to (±)-cannabiorcicyclolic acid[45]. It is important to note that in some cases, **N24** provided slightly superior reaction efficiency, further demonstrating the benefits of using broadly available feedstocks as sensitizers.

In terms of mechanistic understanding, transient absorption spectroscopy, performed using flash laser photolysis with excitation

centred at λ = 355 nm, enabled the observation of the **N34** triplet state, which featured a lifetime of τ = 4.0 µs (Fig. 4c). Stern–Volmer quenching studies further revealed a bimolecular quenching constant of 2.3×10^7 M^{-1} s^{-1} with **27**, confirming its effectiveness as a triplet sensitizer (Fig. 4d,e).

To further demonstrate the potential of $^3\pi,\pi^*$ nitroarenes as photocatalysts, we explored their reactivity in a broader range of EnT transformations. These included intermolecular [2 + 2] cycloadditions involving cinnamate (*E*-**14**) and styrenyl boronate (**37**) as energy acceptors, combined with styrene (**35**) and dimethylbutadiene (**38**) as olefin partners, respectively[47,48]. The resulting cyclobutanes (**36**, **39**) were obtained in good to moderate yields, with high diastereoselectivity. Additionally, triplet excited nitroarenes effectively catalysed the cyclodimerization of cinnamate (*E*-**14**) to afford a tetrasubstituted cyclobutane (**40**) in moderate yield and with excellent stereocontrol[49]. We also applied these photocatalysts in an aza Paternò–Büchi reaction using oxime **41** to deliver the bicyclic azetidine **42** (ref. 50), and in a radical translocation process involving substrate **43** to furnish the corresponding cyclopropane derivative **44** (ref. 51). Collectively, these results highlight the broad synthetic utility of $^3\pi,\pi^*$ nitroarenes in diverse EnT-mediated transformations, reinforcing their potential as versatile and sustainable photocatalysts. In terms of current limitations, we could not extend this reactivity to the sensitization of organometallic complexes, as demonstrated in a dual-catalytic approach for the coupling of aryl bromides and carboxylic acids, where success was not achieved[52].

Conclusions

The field of energy transfer photocatalysis has traditionally focused on designing sensitizers with triplet energies (E_T) closely matching those of the target substrates. Our findings reveal that triplet nitroarenes can act as powerful sensitizers for EnT applications. Crucially, despite having similar E_T values, these species exhibit drastically different reactivity profiles on the basis of their excited-state geometry. This means that excited-state localization can be a crucial factor to consider when approaching the development of novel sensitizers. We demonstrated that nitroarenes with $^3\pi,\pi^*$ configurations display superior catalytic efficiency than their $^3n,\pi^*$ counterparts. This configuration-dependent reactivity highlights the pivotal role of the excited-state electronic configuration, which influences key factors such as lifetimes, transition-state barriers, reorganization barriers and (anti)aromaticity.

Moreover, this work emphasizes the practical and sustainable advantages of using readily available and structurally diverse nitroarenes as photocatalysts. These feedstocks provide an economical and environmentally friendly alternative to traditional sensitizers that rely on precious metals or synthetically complex scaffolds. We hope that this approach will serve as a foundation for the broader identification of feedstock materials, leveraging their excited-state configurations to advance the pursuit of sustainable and efficient photocatalysis.

Methods

General procedure for the *E*-to-*Z* isomerization of alkenes

An oven-dried microwave vial containing a stir-bar was charged with the *E* isomer (1.0 equiv.) and **N24** (5 mol%). The vial was capped with a Supelco aluminium crimp seal with septum (PTFE/butyl) and was evacuated and refilled with argon (×3). Dry and degassed CH_3CN (0.1 M) was added, and the reaction mixture was stirred (>500 r.p.m.) under irradiation with a 390-nm Kessil LED lamp (5-cm distance, 100% intensity, fan on) for the specified time. Quantitative ^{1}H NMR spectroscopy was used to obtain the *E*/*Z* ratio. The solvent was removed under reduced pressure and the residue purified by flash column chromatography to give the pure product.

General procedure for the intramolecular [2 + 2] cycloaddition

An oven-dried microwave vial containing a stir-bar was charged with 1,6-diene (1.0 equiv.) and **N24** or **N34** (10 mol%). The vial was capped with a Supelco aluminium crimp seal with septum (PTFE/butyl) and was evacuated and refilled with argon (×3). Dry and degassed CH_2Cl_2 (0.01 M) was added, and the reaction mixture was stirred (>500 r.p.m.) under irradiation with a 390-nm Kessil LED lamp (5-cm distance, 100% intensity, fan on) for 24 h. Quantitative ^{1}H NMR spectroscopy was used to obtain the ratio of diastereomers. The solvent was removed under reduced pressure and the residue purified by flash column chromatography to give the pure product.

Data availability

The authors declare that the data supporting the findings of this study are available within the paper and its Supplementary Information files. Should any raw data files be needed in another format they are available from the corresponding authors upon reasonable request.

References

1. Hoffmann, N. Photochemical reactions as key steps in organic synthesis. *Chem. Rev.* **108**, 1052–1103 (2008).
2. Holmberg-Douglas, N. & Nicewicz, D. A. Photoredox-catalyzed C–H functionalization reactions. *Chem. Rev.* **122**, 1925–2016 (2022).
3. Dutta, S., Erchinger, J. E., Strieth-Kalthoff, F., Kleinmans, R. & Glorius, F. Energy transfer photocatalysis: exciting modes of reactivity. *Chem. Soc. Rev.* **53**, 1068–1089 (2024).
4. Skubi, K. L., Blum, T. R. & Yoon, T. P. Dual catalysis strategies in photochemical synthesis. *Chem. Rev.* **116**, 10035–10074 (2016).
5. Neveselý, T., Wienhold, M., Molloy, J. J. & Gilmour, R. Advances in the *E*→*Z* isomerization of alkenes using small molecule photocatalysts. *Chem. Rev.* **122**, 2650–2694 (2022).
6. Strieth-Kalthoff, F., James, M. J., Teders, M., Pitzer, L. & Glorius, F. Energy transfer catalysis mediated by visible light: principles, applications, directions. *Chem. Soc. Rev.* **47**, 7190–7202 (2018).
7. Zhou, Q.-Q., Zou, Y.-Q., Lu, L.-Q. & Xiao, W.-J. Visible-light-induced organic photochemical reactions through energy-transfer pathways. *Angew. Chem. Int. Ed.* **58**, 1586–1604 (2019).
8. Dexter, D. L. A theory of sensitized luminescence in solids. *J. Chem. Phys.* **21**, 836–850 (1953).
9. Jiang, Y. & Weiss, E. A. Colloidal quantum dots as photocatalysts for triplet excited state reactions of organic molecules. *J. Am. Chem. Soc.* **142**, 15219–15229 (2020).
10. Liu, Y. et al. Pyrrolo[2,1-*a*]isoquinolines as multitasking organophotocatalysts in chemical synthesis. *Chem. Catal.* **2**, 2726–2749 (2022).
11. Lu, J. et al. Donor–acceptor fluorophores for energy-transfer-mediated photocatalysis. *J. Am. Chem. Soc.* **140**, 13719–13725 (2018).
12. Zhang, Y. et al. Energy-transfer-mediated photocatalysis by a bioinspired organic perylenephotosensitizer HiBRCP. *J. Org. Chem.* **86**, 15284–15297 (2021).
13. Chow, P.-K. et al. Highly luminescent palladium(II) complexes with sub-millisecond blue to green phosphorescent excited states. Photocatalysis and highly efficient PSF-OLEDs. *Chem. Sci.* **7**, 6083–6098 (2016).
14. Zou, Y.-Q. et al. Visible light induced intermolecular [2+2]-cycloaddition reactions of 3-ylideneoxindoles through energy transfer pathway. *Tetrahedron* **68**, 6914–6919 (2012).
15. Ruffoni, A., Hampton, C., Simonetti, M. & Leonori, D. Photoexcited nitroarenes for the oxidative cleavage of alkenes. *Nature* **610**, 81–86 (2022).
16. Wise, D. E. et al. Photoinduced oxygen transfer using nitroarenes for the anaerobic cleavage of alkenes. *J. Am. Chem. Soc.* **144**, 15437–15442 (2022).
17. Hampton, C., Simonetti, M. & Leonori, D. Olefin dihydroxylation using nitroarenes as photoresponsive oxidants. *Angew. Chem. Int. Ed.* **62**, e202214508 (2023).

18. Paolillo, J. M., Duke, A. D., Gogarnoiu, E. S., Wise, D. E. & Parasram, M. Anaerobic hydroxylation of C(sp^3)–H bonds enabled by the synergistic nature of photoexcited nitroarenes. *J. Am. Chem. Soc.* **145**, 2794–2799 (2023).
19. Mitchell, J. K. et al. Photoinduced nitroarenes as versatile anaerobic oxidants for accessing carbonyl and imine derivatives. *Org. Lett.* **25**, 6517–6521 (2023).
20. Matador, E. et al. A photochemical strategy for the conversion of nitroarenes into rigidified pyrrolidine analogues. *J. Am. Chem. Soc.* **145**, 27810–27820 (2023).
21. Mykura, R. et al. Synthesis of polysubstituted azepanes by dearomative ring expansion of nitroarenes. *Nat. Chem.* **16**, 771–779 (2024).
22. Sánchez-Bento, R., Roure, B., Llaveria, J., Ruffoni, A. & Leonori, D. A strategy for *ortho*-phenylenediamine synthesis via dearomative–rearomative coupling of nitrobenzenes and amines. *Chem* **9**, 3685–3695 (2023).
23. Gkizis, P. L., Triandafillidi, I. & Kokotos, C. G. Nitroarenes: the rediscovery of their photochemistry opens new avenues in organic synthesis. *Chem* **9**, 3401–3414 (2023).
24. Mir, M., Jansen, L. M. G., Wilkinson, F., Bourdelande, J. L. & Marquet, J. Efficiency of singlet oxygen generation from the triplet states of nitrophenyl ethers. *J. Photochem. Photobiol. A* **113**, 113–117 (1998).
25. Hurley, R. & Testa, A. C. Triplet-state yield of aromatic nitro compounds. *J. Am. Chem. Soc.* **90**, 1949–1952 (1968).
26. Takezaki, M., Hirota, N. & Terazima, M. Nonradiative relaxation processes and electronically excited states of nitrobenzene studied by picosecond time-resolved transient grating method. *J. Phys. Chem. A* **101**, 3443–3448 (1997).
27. Metternich, J. B. & Gilmour, R. A bio-inspired, catalytic *E*→*Z* isomerization of activated olefins. *J. Am. Chem. Soc.* **137**, 11254–11257 (2015).
28. Murakami, R., Kojima, N., Kamo, R., Tanishima, H. & Inagaki, F. Photoisomerization of alkenes via energy transfer enabled by Cu-acetylide complexes. *Eur. J. Org. Chem.* **26**, e202300948 (2023).
29. Bao, L., Cheng, J.-T., Wang, Z.-X. & Chen, X.-Y. Pyrylium salts acting as both energy transfer and electron transfer photocatalysts for *E*→*Z* isomerization of activated alkenes and cyclization of cinnamic or biaryl carboxylic acids. *Org. Chem. Front.* **9**, 973–978 (2022).
30. Zhan, K. & Li, Y. Visible-light photocatalytic *E* to *Z* isomerization of activated olefins and its application for the syntheses of coumarins. *Catalysts* **7**, 337 (2017).
31. Cruché, C., Neiderer, W. & Collins, S. K. Heteroleptic copper-based complexes for energy-transfer processes: *E*→*Z* isomerization and tandem photocatalytic sequences. *ACS Catal.* **11**, 8829–8836 (2021).
32. Lowry, M. S. et al. Single-layer electroluminescent devices and photoinduced hydrogen production from an ionic iridium(III) complex. *Chem. Mater.* **17**, 5712–5719 (2005).
33. Huang, S. et al. Computational prediction for singlet- and triplet-transition energies of charge-transfer compounds. *J. Chem. Theory Comput.* **9**, 3872–3877 (2013).
34. Frolov, A. N., Kuznetsova, N. A. & El'tsov, A. V. Intermolecular photochemical reduction of aromatic nitro-compounds. *Russ. Chem. Rev.* **45**, 1024–1034 (1976).
35. Wubbels, G. G., Halverson, A. M., Oxman, J. D. & De Bruyn, V. H. Regioselectivity of photochemical and thermal smiles rearrangements and related reactions of β-(nitrophenoxy) methylamines. *J. Org. Chem.* **50**, 4499–4504 (1985).
36. Baird, N. C. Quantum organic photochemistry. II. Resonance and aromaticity in the lowest $^3\pi,\pi^*$ state of cyclic hydrocarbons. *J. Am. Chem. Soc.* **94**, 4941–4948 (1972).
37. Rosenberg, M., Dahlstrand, C., Kilså, K. & Ottosson, H. Excited state aromaticity and antiaromaticity: opportunities for photophysical and photochemical rationalizations. *Chem. Rev.* **114**, 5379–5425 (2014).
38. Yan, J., Slanian, T., Bergman, J. & Ottosson, H. Photochemistry driven by excited-state aromaticity gain or antiaromaticity relief. *Chem. Eur. J.* **29**, e202203748 (2023).
39. Solé-Daura, A. & Maseras, F. Straightforward computational determination of energy-transfer kinetics through the application of the Marcus theory. *Chem. Sci.* **15**, 13650–13658 (2024).
40. Molloy, J. J., Metternich, J. B., Daniliuc, C. G., Watson, A. J. B. & Gilmour, R. Contra-thermodynamic, photocatalytic *E*→*Z* isomerization of styrenyl boron species: vectors to facilitate exploration of two dimensional chemical space. *Angew. Chem. Int. Ed.* **57**, 3168–3172 (2018).
41. Bregent, T., Bouillon, J.-P. & Poisson, T. Photocatalyzed *E*→*Z* contra-thermodynamic isomerization of vinyl boronates with binaphthol. *Chem. Eur. J.* **27**, 13966–13970 (2021).
42. Metternich, J. B. & Gilmour, R. One photocatalyst, *n* activation modes strategy for cascade catalysis: emulating coumarin biosynthesis with (−)-riboflavin. *J. Am. Chem. Soc.* **138**, 1040–1045 (2016).
43. Juliá, F., Constantin, T. & Leonori, D. Applications of halogen-atom transfer (XAT) for the generation of carbon radicals in synthetic photochemistry and photocatalysis. *Chem. Rev.* **122**, 2292–2352 (2022).
44. Poplata, S., Tröster, A., Zou, Y.-Q. & Bach, T. Recent advances in the synthesis of cyclobutanes by olefin [2+2] photocycloaddition reactions. *Chem. Rev.* **116**, 9748–9815 (2016).
45. Lu, Z. & Yoon, T. P. Visible light photocatalysis of [2+2] styrene cycloadditions by energy transfer. *Angew. Chem. Int. Ed.* **51**, 10329–10332 (2012).
46. Mojr, V. et al. Flavin photocatalysts for visible-light [2+2] cycloadditions: structure, reactivity and reaction mechanism. *ChemCatChem* **10**, 849–858 (2018).
47. Pagire, S. K., Hossain, A., Traub, L., Kerres, S. & Reiser, O. Photosensitised regioselective [2+2]-cycloaddition of cinnamates and related alkenes. *Chem. Commun.* **53**, 12072–12075 (2017).
48. Liu, Y. et al. M. K. Photosensitized [2+2]-cycloadditions of alkenylboronates and alkenes. *Angew. Chem. Int. Ed.* **61**, e202200725 (2022).
49. Lei, A. et al. General and efficient intermolecular [2+2] photodimerization of chalcones and cinnamic acid derivatives in solution through visible-light catalysis. *Angew. Chem. Int. Ed.* **56**, 15407–15410 (2017).
50. Becker, M. R., Richardson, A. D. & Schinder, C. S. Functionalized azetidines via visible light-enabled aza Paternò–Büchi Reactions. *Nat. Comm.* **10**, 5095 (2019).
51. Zheng, Y., Dong, Q.-X., Wen, S.-Y., Ran, H. & Huang, H.-M. Di-π-ethane rearrangement of cyano groups via energy-transfer catalysis. *J. Am. Chem. Soc.* **146**, 18210–18217 (2024).
52. Welin, E. R., Le, C., Arias-Rotondo, D. M., McCusker, J. K. & MacMillan, D. W. C. Photosensitized, energy transfer-mediated organometallic catalysis through electronically excited nickel(II). *Science* **355**, 380–385 (2017).

Acknowledgements

D.L. acknowledges the European Research Council for a grant (101086901) and the Deutsche Forschungsgemeinschaft for a grant (LE 5124/1-1). E.M.A. thanks the Marie Skłodowska-Curie Actions for a fellowship (101150311). B.K. thanks the European Union Horizon 2020 innovation programme under Marie Skłodowska-Curie grant agreement number 956324 (PhotoReAct). We gratefully acknowledge the computing time provided to them at the NHR Center NHR4CES at RWTH Aachen University (project number p0021519). This is funded

by the Federal Ministry of Education and Research, and the state governments participating on the basis of the resolutions of the GWK for national high-performance computing at universities (www.nhr-verein.de/unsere-partner). R. Gilmour (University of Münster) is acknowledged for useful discussions.

Author contributions

D.L. designed and supervised the project. M.R., B.K. and P.T.B. performed all synthetic work. E.M.A. performed all computational work. M.R., B.K., P.T.B., A.R., E.M.A. and D.L. analysed the results and wrote the paper.

Funding

Open access funding provided by RWTH Aachen University.

Competing interests

The authors declare no competing interests.

Additional information

Supplementary information The online version contains supplementary material available at https://doi.org/10.1038/s41929-025-01453-z.

Correspondence and requests for materials should be addressed to Enrique M. Arpa or Daniele Leonori.

Peer review information *Nature Catalysis* thanks Christoforos Kokotos, Wen-Jing Xiao and the other, anonymous, reviewer for their contribution to the peer review of this work.